SPACE WEATHER, VOL. 6, S07005, doi:10.1029/2007SW000343, 2008

Calculation of geomagnetically induced currents in the 400 kV power grid in southern Sweden

M. Wik,[1,2] A. Viljanen,[3] R. Pirjola,[3] A. Pulkkinen,[4,5] P. Wintoft,[1] and H. Lundstedt[1]

Received 13 June 2007; revised 12 April 2008; accepted 25 April 2008; published 31 July 2008.

[1] Sweden has experienced many geomagnetically induced current (GIC) events in the past, which is obviously due to the high-latitude location of the country. The largest GIC, almost 300 A, was measured in southern Sweden in the earthing lead of a 400 kV transformer neutral during the magnetic storm on 6 April 2000. On 30 October 2003, the city of Malmö at the southern coast suffered from a power blackout caused by GIC, leaving 50,000 customers without electricity for about 20–50 min. We have developed a model that enables calculation of GIC in the southern Swedish 400 kV power grid. This work constitutes the first modeling effort of GIC in Sweden. The model is divided into two parts. The electric field is first derived using a ground conductivity model and geomagnetic recordings from nearby stations. The conductivity model is determined from a least squares fit between measured and calculated GIC. GIC are calculated using a power grid model consisting of the topology of the system and of the transformer, transmission line, and station earthing resistances as well as of the coordinates of the stations. To validate the model, we have compared measured and calculated GIC from one site. In total, 24 events in 1998 to 2000 were used. In general the agreement is satisfactory as the correct GIC order of magnitude is obtained by the model, which is usually enough for engineering applications.

Citation: Wik, M., A. Viljanen, R. Pirjola, A. Pulkkinen, P. Wintoft, and H. Lundstedt (2008), Calculation of geomagnetically induced currents in the 400 kV power grid in southern Sweden, *Space Weather*, *6*, S07005, doi:10.1029/2007SW000343.

1. Introduction

[2] Geomagnetically induced currents (GIC) are the ground end of the space weather chain that originates at the Sun. During a geomagnetic storm, intense currents are produced in the magnetosphere and ionosphere creating time-dependent magnetic fields. At the Earth's surface, a geoelectric field is induced as expressed by Faraday's law of induction. The electric field drives currents in the ground and in man-made technological conductor networks, such as power grids, oil and gas pipelines, telecommunication cables, and railway equipment [e.g., *Pirjola*, 2000]. This paper focuses on power grids.

[3] GIC enter a power grid through earthed transformer neutrals ("earthing currents") and flow along transmission lines ("line currents") to other transformers, at which they go back to the ground. A GIC path between two transformers is shown in Figure 1. The characteristic times of GIC and geoelectromagnetic fields vary from seconds to days with 1 Hz regarded as the upper limit of the relevant frequencies involved. GIC flowing in power grids are thus DC-like compared to the 50/60 Hz frequency used for electricity. When GIC flow in transformer windings, a DC magnetic field is created that can saturate the core. This leads to a nonlinear operation of the transformer [e.g., *Kappenman and Albertson*, 1990; *Kappenman*, 1996; *Bolduc*, 2002; *Molinski*, 2002; *Lindahl*, 2003, and references therein]. The magnetizing current much increases during every half-cycle resulting in an excessive amount of harmonics. Protective relays may suffer from malfunction and parts of the system can be disconnected. Together with increased reactive power demands these effects may cause a collapse of the whole system. The most famous GIC event is the blackout in Québec, Canada, in March 1989 [e.g., *Bolduc*, 2002]. In a saturated transformer, the magnetic flux can spread out through structural members producing eddy currents, which in turn may cause hotspots possibly with permanent damage.

[4] In theory, GIC problems may be avoided by trying to block the flow of GIC by series capacitors or to decrease the magnitudes of GIC by additional resistances, also provided, e.g., by reactors in transformer neutral leads.

[1]Swedish Institute of Space Physics, Lund, Sweden.
[2]Department of Physics, Lund University, Lund, Sweden.
[3]Finnish Meteorological Institute, Helsinki, Finland.
[4]NASA Goddard Space Flight Center, Greenbelt, Maryland, USA.
[5]Goddard Earth Sciences and Technology Center, University of Maryland, College Park, Maryland, USA.

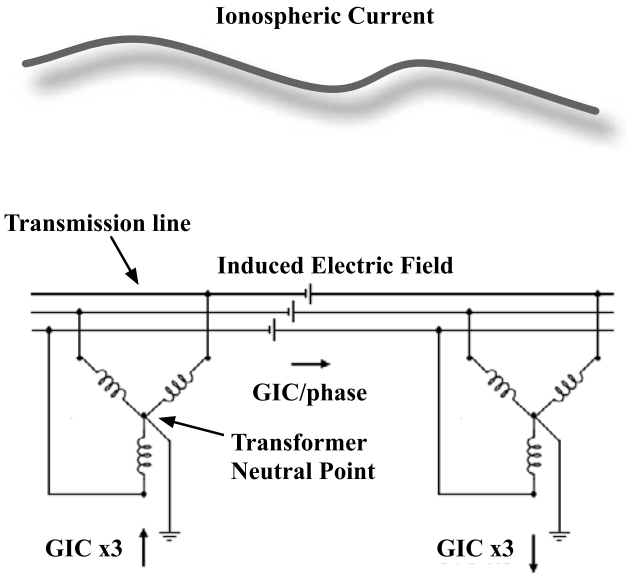

Figure 1. Geomagnetically induced currents (GIC) flowing along the transmission line between two transformers. A time-varying ionospheric current, i.e., the primary driver of GIC, is also schematically shown.

However, studies show that unless the locations are very carefully chosen, such devices may in fact increase GIC and the risks [*Erinmez et al.*, 2002a; *Pirjola*, 2002, 2005a]. Another approach to mitigate GIC effects is to use forecasting and nowcasting techniques of space weather events, so that the users of the systems may take suitable protective actions.

[5] GIC are mainly (but not only) a high-latitude phenomenon. Sweden has experienced many GIC problems in power systems [e.g., *Elovaara et al.*, 1992] as well as in telecommunication systems [e.g., *Karsberg et al.*, 1959] and even on railways [*Wallerius*, 1982]. A well-known GIC event is the power blackout in the city of Malmö at the southern coast of Sweden on 30 October 2003 [*Lindahl*, 2003; *Pulkkinen et al.*, 2005]. This outage affected 50,000 customers and lasted between 20 and 50 min. Furthermore, the largest measured GIC value that to our knowledge has ever been reported also refers to Sweden, where a current of almost 300 A, i.e., 100 A per phase, was measured in the earthing lead of a 400 kV transformer at the eastern coast of southern Sweden on 6 April 2000 [*Erinmez et al.*, 2002b].

[6] In spite of the many GIC problems that the Swedish high-voltage power grid has experienced, modeling of GIC in the system has not been performed until now. During the recent ''Space Weather Applications Pilot Project'' of the European Space Agency (ESA) a real-time forecast service for GIC was developed [*Wintoft*, 2005; *Lundstedt*, 2006]. In this paper we present results of model calculations of GIC in the southern Swedish 400 kV power grid, together with comparisons to measured GIC data at one site. Before a discussion of examples for several events (section 3), we summarize the GIC calculation technique (section 2) that includes geomagnetic data and network parameters as the input.

2. Calculation of GIC in a Power Grid

[7] Modeling of GIC in a power grid (or any other network) is conveniently divided into two independent steps: (1) calculation of the horizontal geoelectric field and (2) computation of GIC using this field. These two steps are usually referred to as the ''geophysical step'' and the ''engineering step.'' The former is more difficult since, in principle, it requires knowledge of magnetospheric-ionospheric currents and the Earth's conductivity distribution, both of which are complicated and not known accurately. On the basis of Maxwell's equations and boundary conditions, *Häkkinen and Pirjola* [1986] present exact formulas for calculating the electric and magnetic fields at the surface of a layered Earth due to a general three-dimensional magnetospheric-ionospheric current system. Numerical computations to perform the geophysical step are however laborious and slow. *Viljanen et al.* [2004] show that in practice the most appropriate method to determine the geoelectric field is to use ground-based geomagnetic data and the plane wave relation between the horizontal electric and magnetic fields at the Earth's surface:

$$E_x(\omega) = Z(\omega)B_y(\omega)/\mu_0,\ E_y(\omega) = -Z(\omega)B_x(\omega)/\mu_0 \qquad (1)$$

where $Z(\omega)$ is the (local) surface impedance and μ_0 is the vacuum permeability. The x and y axes point to the north and east, respectively. The impedance $Z(\omega)$ depends on the angular frequency ω and characterizes the Earth's conductivity structure. The use of equation (1) thus requires a Fourier transform between the time (t) and frequency (ω) domains. Usually, measured geomagnetic data are not available from a dense array of stations. Therefore the data have to be interpolated onto a grid covering the network (see Figure 2). This can be done by utilizing the Spherical Elementary Current System (SECS) method, which first includes the determination of equivalent ionospheric currents based on magnetic recordings [*Amm*, 1997; *Pulkkinen et al.*, 2003]. The magnetic field produced by these currents can then be computed at any point on the ground.

[8] The engineering step is more straightforward and can in principle be carried out exactly based on Ohm's and Kirchhoff's laws and on Thévenin's theorem. Owing to the low frequencies compared to 50/60 Hz, a dc treatment is sufficient. *Lehtinen and Pirjola* [1985] derive the formula

$$I_e = (U + Y_n Z_e)^{-1} J_e \qquad (2)$$

for the $N \times 1$ matrix I_e consisting of GIC flowing into the Earth at the N earthing points of the power grid considered. In equation (2), U is the $N \times N$ unit matrix and Y_n and Z_e are the $N \times N$ network admittance matrix

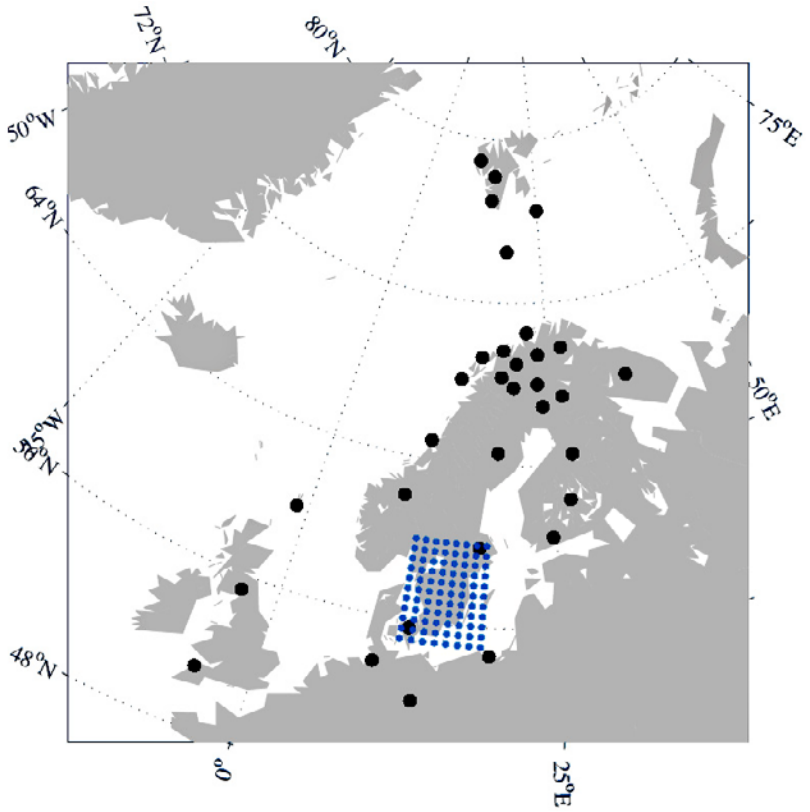

Figure 2. Magnetometer observatories (black) and a dense grid for the interpolation (blue). The observatories in the SW and NE corners of the grid are Brorfelde and Uppsala.

and the $N \times N$ earthing impedance matrix, respectively. The matrices Y_n and Z_e are real and depend on the resistances in the system. The $N \times 1$ matrix J_e involves the (geo)voltages obtained by integrating the geoelectric field along the paths defined by the transmission lines in the power grid. It is important to stress that the geoelectric field is generally rotational. This means that no single valued potential at the Earth's surface exists and the induced voltage between any two points depends on the integration path of the electric field [e.g., *Pirjola*, 2000]. The driver, or "battery," for GIC must then be treated as induced voltages in the transmission lines and not in the ground [*Boteler and Pirjola*, 1998]. A power system uses three-phase conductors. GIC flowing in a network will be divided equally between the phases. When calculating GIC, all three phases are therefore convenient to be handled as one conductor with a resistance of one third of that of a single phase.

3. Calculation of GIC in the 400 kV Power Grid

[9] We will consider the 400 kV system in southern Sweden with special attention to the site Simpevarp-2 (site 21 in Figure 3), at which GIC is recorded. To calculate GIC, we need the geoelectric field together with resistance, configuration and coordinate data of the whole power network (Figure 3).

[10] GIC have been recorded in the Swedish 400 kV power system since 1998. The recordings take place at a transformer neutral, Simpevarp-2 (site 21 in Figure 3), at the east coast close to the nuclear power plant OKG in Oskarshamn. In this study we refer to measured GIC data, recorded instantaneously every minute, from 1998 to 2000. At the end of 2000, a resistor was installed in the earthing lead of the transformer neutral of Simpevarp-2 to decrease GIC. Therefore it is not reasonable to include data later than 2000 in this study. The coordinates for OKG and the measurement site are approximately 57.4 N and 16.7 E.

[11] We start with an empirical approach and then present results by the full modeling. As a measure of success, we use the relative error, RE (%), between the measured (GIC_{meas}) and modeled GIC (GIC_{mod}) defined by

$$RE = 100 \cdot |GIC_{meas} - GIC_{mod}|/|GIC_{meas}| \quad (3)$$

where all timesteps with $|GIC_{meas}|$ exceeding a given threshold are included. We also use the linear correlation between measured and modelled GIC.

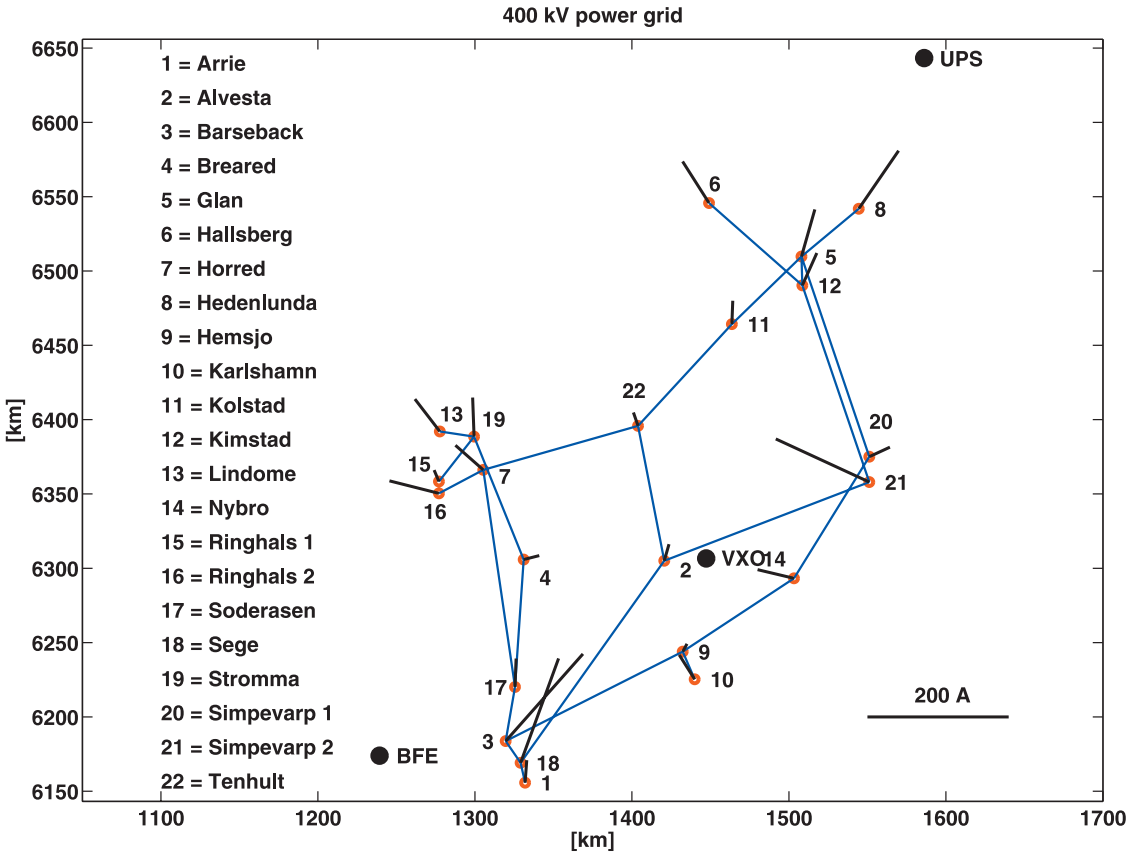

Figure 3. Southern Swedish 400 kV power grid model. The coordinates for Ringhals 1 and 2 and Simpevarp 1 and 2 are modified to better resolve them on the map. GIC is recorded at Simpevarp-2 (site 21). The black line segment gives the direction of a uniform electric field (1 V/km) which creates the largest GIC at each station. The amplitude of GIC is proportional to the length of the line segment. At Simpevarp-2, the maximum GIC is reached if the electric field points to, or from, west-northwest. The magnetic observatories, Brorfelde (BFE) and Uppsala (UPS), are also shown together with the new magnetometer station in Växjö (VXO) being installed into operation. The coordinates are given in the RT90 reference system.

3.1. Empirical Relation Between the Electric Field and GIC

[12] It is possible to try to relate the measured GIC directly to the modeled electric field without the DC description of the power grid. The simplest assumption is that the electric field is spatially uniform. Then GIC is simply:

$$GIC(t) = \alpha E_x(t) + \beta E_y(t) \tag{4}$$

where (E_x,E_y) are the modeled values close to the GIC site. The electric field is determined from a model of the Earth's conductivity. This is described in more detail in section 3.2.2. The coefficients (α,β) are determined by a least squares fit. Table 1 shows examples of the values. As seen, the ratio β/α depends on the selected threshold value of GIC as well as on the location of the point where the electric field is calculated. The ratio varies between -1.5 and -4.9, and its absolute value decreases with an increasing GIC threshold.

[13] The empirical approach is valid only for the specific GIC site with an additional assumption that the power grid remains unchanged. Consequently, the preferred modeling method is to use the DC description.

3.2. Full Network Modeling

[14] The full network GIC model is divided into a power grid model and an electric field model. We start with the power grid model and a comparison with the results in the previous section. We then determine the Earth's conductivity, in the electric field model, by comparing measured and modeled GIC.

3.2.1. 400 kV Power Grid

[15] The full approach requires a DC model of the power grid. The power grid data were obtained from

Table 1. Empirical Coefficients (α,β) From Equation (4)[a]

α	β	corr	MRE	GIC_0	long/lat	N
−31.0	137.5	69.6	56.3	5	16/57	3372
−28.9	137.3	69.6	56.3	5	17/57	3372
−31.7	134.2	69.6	56.3	5	16/57.5	3372
−28.8	134.1	69.6	56.3	5	17/57.5	3372
−59.3	151.5	72.7	53.5	10	16/57	1493
−54.9	152.1	72.7	53.5	10	17/57	1493
−57.7	147.6	72.7	53.5	10	16/57.5	1493
−52.5	148.3	72.7	53.5	10	17/57.5	1493
−94.2	163.2	74.9	52.5	15	16/57	843
−87.4	164.7	74.9	52.5	15	17/57	843
−90.4	158.8	74.9	52.5	15	16/57.5	843
−82.8	160.2	74.9	52.5	15	17/57.5	843
−113.0	171.9	76.1	54.0	20	16/57	554
−103.5	173.9	76.1	54.0	20	17/57	554
−107.6	167.6	76.1	54.0	20	16/57.5	554
−97.4	169.4	76.1	54.0	20	17/57.5	554

[a]Correlation between measured and modeled geomagnetically induced currents (GIC) is given by corr. The median relative error (%) between measured and modeled GIC is given by MRE. GIC_0 is the threshold value in amperes of measured GIC taken into account, long/lat is the electric field grid point in longitude and latitude, and N gives the number of available timesteps.

Svenska Kraftnät, SVK. They include the network topology, station coordinates, transformer resistances, transmission line resistances, and station earthing resistances. At some stations the 400 kV network is connected to the 130 kV system by autotransformers. The effect of autotransformers on GIC in the 400 kV system is approximately taken into account by decreasing the corresponding earthing resistance values. The grid considered contains 22 stations and 24 lines (Figure 3). We assume the lines to be straight between the stations. However, their correct resistance values, which take into account the real lengths of the lines, are used.

[16] To get a general idea about the distribution of GIC in the network, we first calculated GIC due to a uniform electric field of 1 V/km having any direction. In such a case, GIC is obtained from the electric field by

$$GIC(t) = a \cdot E_x(t) + b \cdot E_y(t) \quad (5)$$

where the multipliers (a,b) can be calculated based on the power grid data. Figure 3 shows the field directions that give the largest GIC, proportional to the black line segment, at each station. The scaling in the figure corresponds to the electric field magnitude 1 V/km. It is clear from the figure that the largest GIC are found at the corners and ends of the network [cf. *Viljanen and Pirjola*, 1994], and the sites most prone to experience large GIC can be identified.

[17] The coefficients of equation (5) for Simpevarp-2 are (a,b) = (−62.2,133.2) Akm/V. So the ratio b/a is about −2, which should be compared to the empirical ratio β/α. In an ideal case of a uniform electric field and a completely described power grid, these two ratios should be equal. We emphasize that (α,β) in equation (4) are not necessarily equal to (a,b) in equation (5). The former depend on both the power grid data and the selected conductivity model, whereas the latter depend only on the power grid data.

[18] There are some differences between the two approaches, whose explanations are as follows: The electric field is not spatially uniform in the whole power grid. Additionally, the closest magnetic observatories are quite distant, so the electric field calculated close to Simpevarp has some uncertainty. We will discuss the DC modeling problems in more detail in section. 3.4.

3.2.2. Geoelectric Field Model

[19] The next step in the full approach is to determine the model of the Earth's conductivity. This is performed by comparing the measured GIC to the modeled one.

[20] The geomagnetic field is recorded continuously at several sites in northern Europe. In this study we use stations in and near Sweden. They include all IMAGE magnetometer array sites and seven INTERMAGNET stations. By applying the SECS method, the geomagnetic data, with 1-min resolution, were interpolated to a dense grid, covering the area of the power grid (Figure 2). The surface electric field was then calculated, using equation (1), by multiplying the interpolated geomagnetic field by the surface impedance at each grid point.

[21] In the initial model, the Earth was uniform having the resistivity 40 Ωm. The resistivity was then optimized using a correction factor calculated from a least squares fit between measured and calculated GIC. With the correction factor equal to 1, the new value for the resistivity was 550 Ωm. This value was then used as a starting point for a second model consisting of two layers (one layer above a half-space). A table consisting of several hundred combinations of thicknesses and resistivities was then used to calculate, for each combination, the above correction factor again, together with the median relative error and the sum of the absolute errors. The final model, or combination, was based on a correction factor very close to 1, a low median error and a low sum of absolute errors. The final conductivity model has a thickness of 230 km, a resistivity of the upper layer 800 Ωm and a resistivity of the lower layer 250 Ωm (which we term 230/800/250). This is mainly in agreement with magnetotelluric measurements in southern Sweden (G. Schwarz, Swedish Geological Survey, private communication, 2007).

[22] It should be noted that in GIC calculations the geoelectric field is integrated along power transmission lines, so small horizontal details in the scale of 10 km or less of the ground conductivity can be neglected. A two-layer ground model has been used successfully for southern Finland as well [*Viljanen et al.*, 2006]. Here we assume that the same conductivity model can be used in the whole region of study. The simplest choice would be a uniform Earth only. However, the lower layer with a larger conductivity simulates better the general increase of the conductivity as a function with depth.

Table 2. Events Used in This Study[a]

	Event	Values	Maximum $\|GIC\|$	Correlation
01	19980924	35	38	0.40
02	19980925	472	77	0.67
03	19981002	82	25	0.34
04	19990815	63	19	0.91
05	19990820	53	24	0.80
06	19990830	21	21	0.83
07	19990922	207	73	0.86
08	19990926	52	19	0.81
09	19991010	53	27	0.67
10	19991012	73	25	0.23
11	19991022	310	67	0.64
12	19991028	42	29	0.68
13	20000122	49	30	0.66
14	20000224	90	19	0.68
15	20000406	321	269	0.55
16	20000523	71	31	0.90
17	20000608	290	63	0.70
18	20000710	22	23	0.91
19	20000711	77	44	0.79
20	20000713	129	21	0.71
21	20000714	147	49	0.92
22	20000715	469	222	0.81
23	20000719	12	39	0.43
24	20000812	232	34	0.76

[a]Listed in the table are the day of the event, number of values with $|GIC| > 5$ A, measured maximum $|GIC|$, and correlation between measured and calculated GIC. There are, in total, 3372 values used.

[23] Using equation (2), we then calculated GIC at Simpevarp-2 for 24 events in 1998 to 2000, i.e., at the previous sunspot maximum. The 24 events used here are listed in Table 2. The results, obtained by using the 230/800/250 model, for three of these events are shown in Figure 4. Also listed in the table are the correlation coefficients for measured (above 5 A) and modeled GIC for each event.

3.3. Error Analysis

[24] In this study we used data points with measured $|GIC| > 5$ A. The total number of values for all 24 events are then equal to 3372.

[25] The median relative error between measured and calculated GIC is 56.4 percent. For these events the correlation between measured and calculated GIC is about 0.7 (Figure 5).

[26] We then examined the relationship between the relative error and measured GIC. For practical applications it is significant to know if large relative errors tend to occur at large or small measured GIC values. Figure 6 shows that the relative error is smaller for large values of measured GIC, and vice versa, which is good for practical applications.

[27] For all events, in general, the modeled GIC follows qualitatively well the measured one, but there are times when the deviations in magnitude are quite large, e.g., for

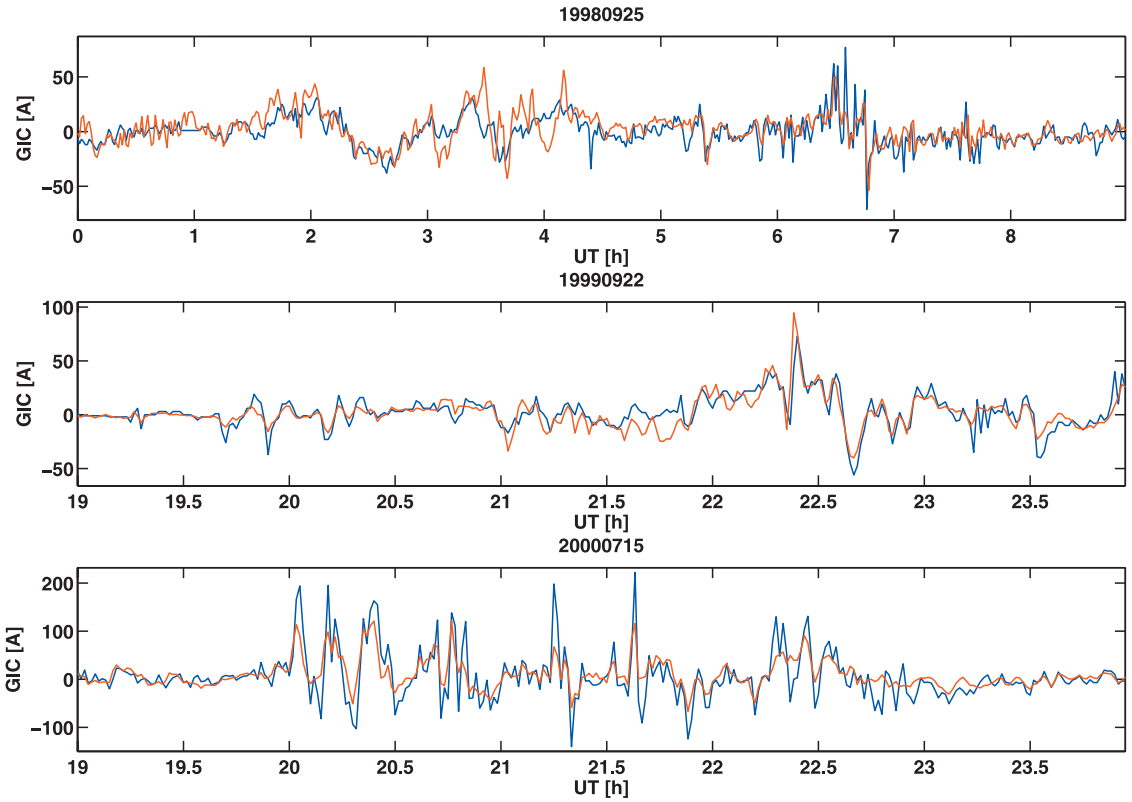

Figure 4. Measured (blue) and calculated (red) GIC at Simpevarp-2 for three events in 1998 to 2000.

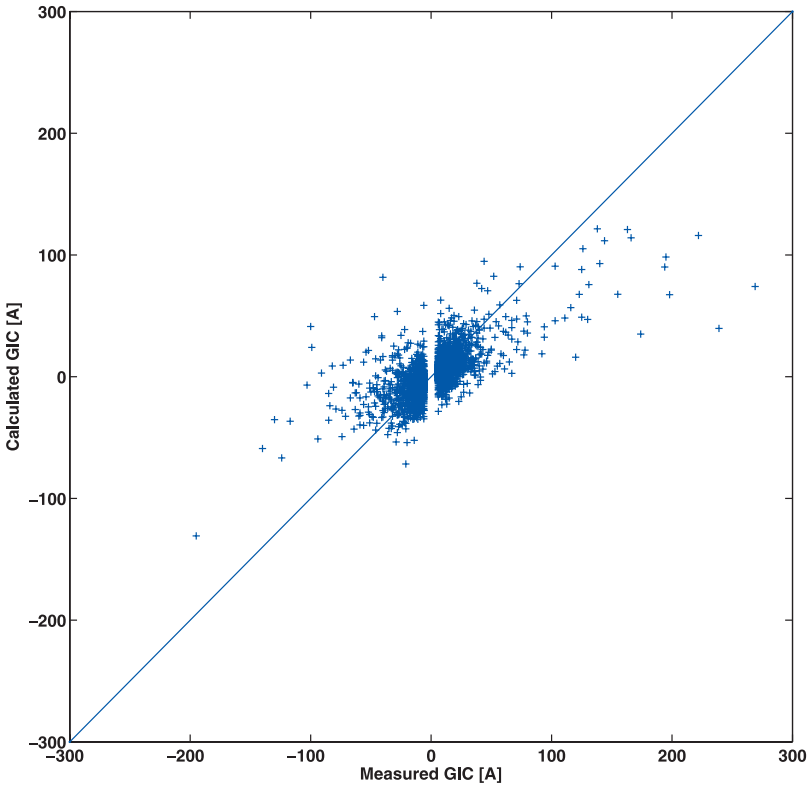

Figure 5. Calculated GIC (equation (5)) as a function of measured GIC at Simpevarp-2. The straight line indicates a perfect fit between measured and calculated GIC. The correlation is about 0.7. Data points with the absolute value of the measured GIC exceeding 5 A are considered. The total number of values is 3372.

the 6 April 2000 event. A possible reason for these differences is the large distance from Simpevarp-2 to the nearest magnetic observatory. In this study the closest magnetic observatories (Uppsala and Brorfelde) are situated about 280 km north of and 360 km southwest of the GIC measurement site, respectively. The variation of the magnetic field with latitude will therefore not be captured exactly [*Viljanen et al.*, 2004; *Pulkkinen et al.*, 2007].

[28] We examine the 6 April 2000 event (Figure 7) in some more detail. At the start of this event, the modeled GIC is in good agreement with the measured GIC, but later on the difference between them increases. One possibility is that the calculated geoelectric field does not capture the variation of the magnetic field at the end of the event.

[29] We therefore examined the magnetic field data from Uppsala and Brorfelde. The correlation for the magnetic field, B_x, between Uppsala and Brorfelde is about 0.9. This means that the magnetic field is rather homogenous during the event. The correlation for the derivative of the magnetic field, dB_x/dt, is, however, only 0.1. The magnetic field variation, dB_x/dt, is shown in the lower part of Figure 7. The negative of the derivative, $-dB_x/dt$, is related to the eastward geoelectric field [*Viljanen et al.*, 2001]. The geomagnetic variation is therefore a good indicator of the electric field and GIC at Simpevarp.

[30] Since Simpevarp is located about halfway between Uppsala and Brorfelde, it is reasonable to assume that the variation of the interpolated magnetic field, and therefore the electric field, close to Simpevarp-2, will have some degree of uncertainty. However, by comparing the measured GIC with dB_x/dt from Uppsala and Brorfelde, we see that the highest values of the derivative also occur when we have the highest values of GIC. It is likely that we would achieve a better agreement by using a 2-D/3-D conductivity model in combination with measurements of the magnetic field closer to Simpevarp. However, the use of such conductivity models would require much more CPU time, so they would be quite impractical in studies of long time series.

[31] For testing purposes of the effects of the time resolution we also calculated GIC based on 10 s geomagnetic data from Uppsala during the same event. Since we only used data from one magnetometer station, there is no interpolation of the magnetic field. Instead we choose the magnetic field from Uppsala to be the same all over the

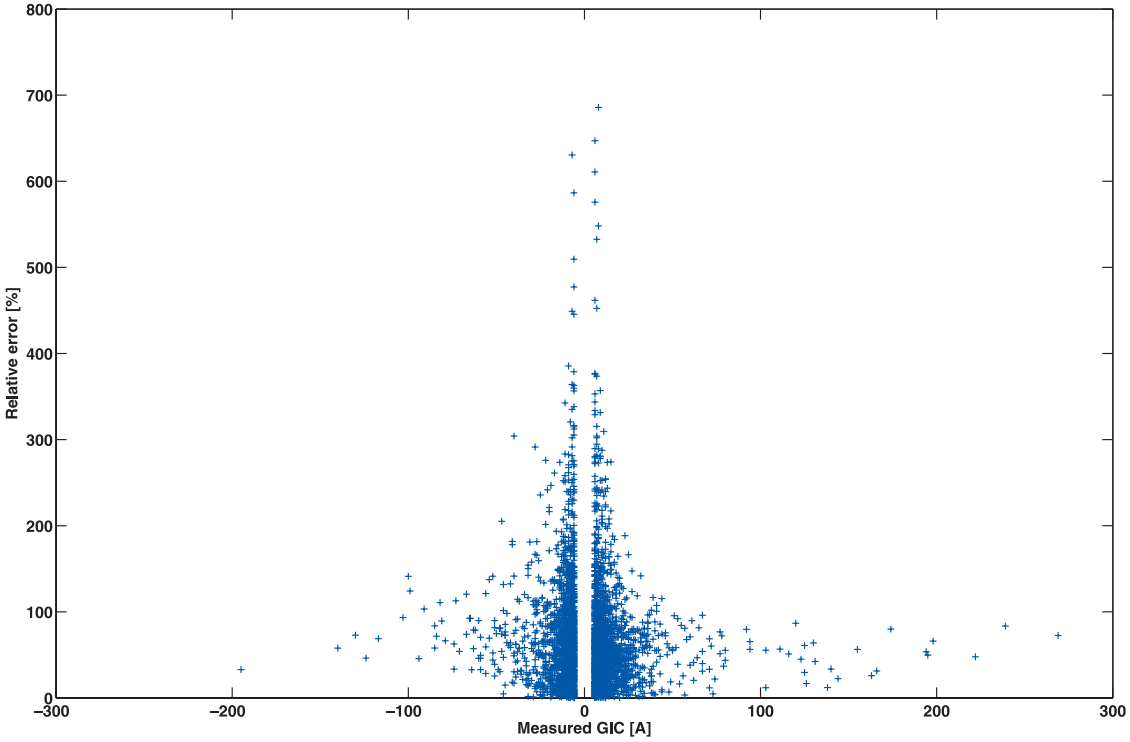

Figure 6. The relative error as a function of measured GIC at Simpevarp-2. Data points with the absolute value of the measured GIC exceeding 5 A are considered.

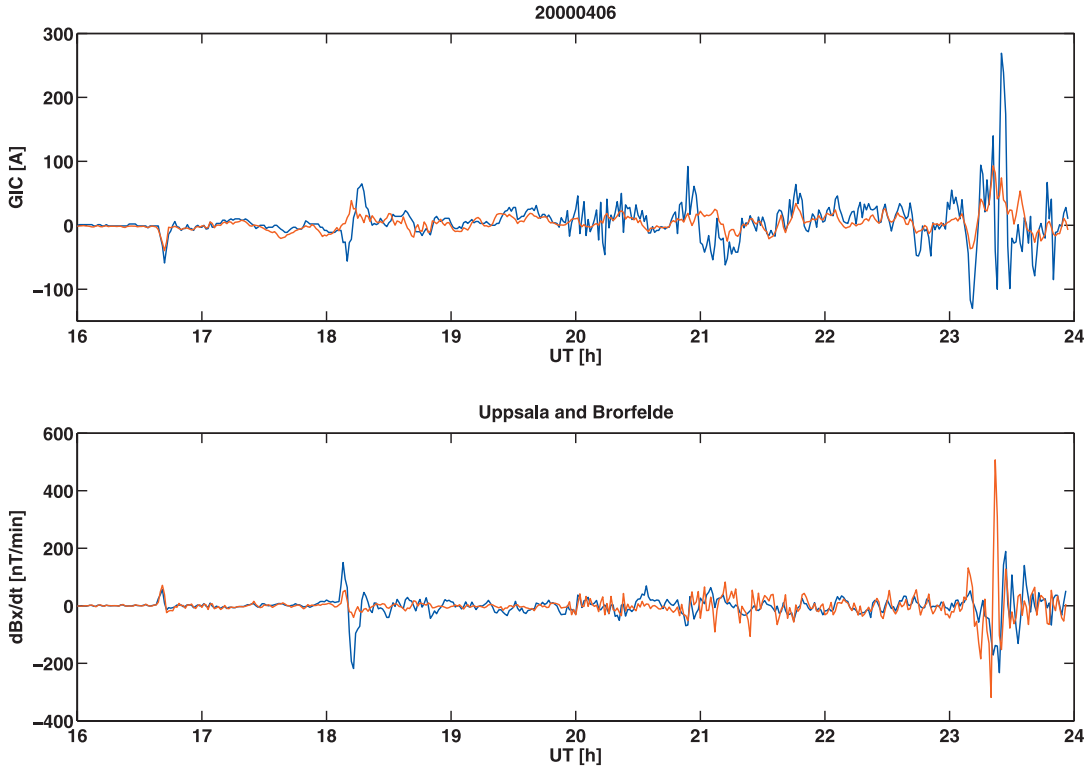

Figure 7. The top curve shows the measured (blue) and calculated (red) GIC at Simpevarp-2 (6 April 2000). The bottom curve shows dB_x/dt from Uppsala (blue) and Brorfelde (red).

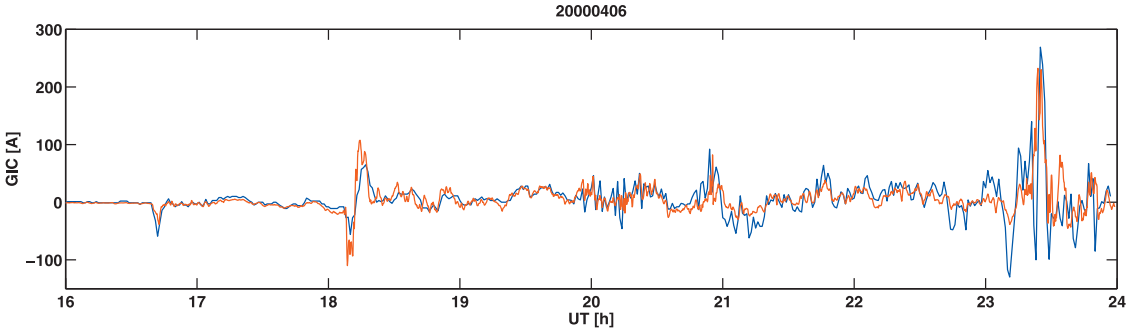

Figure 8. Measured (blue) and calculated (red) GIC at Simpevarp-2 (6 April 2000). Calculated GIC has a resolution of 10 s.

grid. The electric field was then calculated as before. The results are shown in Figure 8. In this case the calculated GIC correlates better with measured GIC. Using the same time stamps, we achieve a correlation of 0.59 between 1 min measured GIC and 10 s calculated GIC. Although not conclusive, this indicates that at times it might be necessary to use higher time resolution for the geomagnetic field. Unfortunately, 10 s data are not available for all magnetometer stations in the period 1998–2000. However, the use of 10 s data, for both GIC and geomagnetic data, should be considered for future studies.

[32] The results presented in this paper should also be compared with the nowcasting service of the Finnish natural gas pipeline system. In that study the distance between the GIC measurement site and the magnetic observatory is only about 30 km, giving a median error of about 30% [*Viljanen et al.*, 2006].

3.4. About Errors Caused by Deficiencies in the Power Grid Model

[33] In principle, the engineering step of a GIC calculation can be performed exactly based on Ohm's and Kirchhoff's laws and Thévenin's theorem and by combining geoelectric data with the power grid model, which includes the resistance values and the configuration of the system. In practice, however, power grid data are never perfect, and so GIC calculations necessarily involve approximations. The values of station earthing resistances provided by power companies usually refer to measured 50/60 Hz ac data while dc resistances are needed for GIC computations. Furthermore, earthing resistances of some stations often even remain completely unknown and thus have to be replaced by average estimates. Effects of networks with voltages less than 400 kV, not included in the present study, are approximated by changing the effective earthing resistances met by GIC at stations with autotransformers. These problems with earthing resistances are, however, not important in practice since the impacts of uncertainties in those data on GIC have been shown to be insignificant [e.g., *Kappenman et al.*, 1981, p. 4–10; *Pirjola*, 2008].

[34] Larger and more serious errors may occur in the calculation of GIC if possible additional resistances in earthing leads of transformer neutrals or some transmission lines are excluded from the power grid model. *Pirjola* [2005b] has shown that when focusing on GIC at a particular site it is sufficient to consider a smaller grid in the vicinity of the site. Therefore, regarding GIC at Simpevarp-2, only stations in the eastern part of the power grid and lines entering Simpevarp-2 are important to be modeled correctly. We are not able to extract completely certain and precise information about all details and about possible temporary changes in the southern Swedish 400 kV grid from the power company, so this may be a reason for some of the discrepancies between measured and computed GIC data. However, in general, our calculations of GIC can obviously be considered correct and reliable.

4. Discussion and Conclusions

[35] Geomagnetically induced currents constitute the ground end of the space weather chain. They have been known since the mid-1850s, i.e., for a much longer time than the actual history of modern space weather research. GIC are a potential source of problems to technological systems. Today electric power transmission systems, discussed in this paper, are the most important regarding GIC, which can saturate transformers with harmful consequences extending from an increased harmonic content in the electric power to a blackout of the entire network and permanent damage of transformers. Several GIC events and effects on the power system have occurred in Sweden in the past.

[36] On the basis of theoretical modeling and measured data, this paper provides an analysis of GIC in the southern Swedish 400 kV system, and is thus the first quantitative modeling of GIC in Sweden. The input used in the study consists of magnetic data from several sites in northern Europe, especially from Brorfelde, Denmark, and Uppsala, Sweden, located southwest and northeast of the network, of power grid data and of GIC recordings

in the Simpevarp-2 transformer neutral at the eastern edge of the network.

[37] Altogether 24 GIC events in 1998 to 2000 are investigated in this paper. After adjusting the initial conductivity model, a satisfactory agreement between modeled and measured GIC at Simpevarp-2 is obtained. For other sites, where GIC recordings are not available, we cannot estimate the accuracy of the model. However, for Simpevarp-2, the accuracy of the calculations is sufficient for practical purposes in which the levels of GIC rather than precise values should be known.

[38] A specific storm studied separately in this paper occurred on 6 April 2000, during which an extremely large GIC of almost 300 A was measured at Simpevarp-2. This is, as far as we know, the largest measured GIC ever reported. However, in this case the modeled GIC much differs from the measured data. A probable reason for this is that the calculated electric field is too smooth or that the time resolution is too low during the most extreme part of the event. This conclusion is in agreement with the results shown in Figure 8. It is also of interest to see that the modeled GIC appears to be systematically lower then the measured GIC, at least for larger GIC values (Figure 5). The large number of small GIC values makes a bias to the fit so that the results underestimate large GIC. This deviation becomes less prominent if we use a larger threshold for GIC. In general, we suspect that the largest GIC values are related to the most rapid magnetic field variations which are not captured by the 1 min data. For this reason, 10 s data of the magnetic field should be considered in future studies. Other reasons could be effects of the lower voltage systems, not included in the calculation, or some changes in the power grid configuration occurring every now and then.

[39] *Viljanen et al.* [2004] show that the spatial variation of the electric field due to the corresponding variation of ionospheric currents is rather uniform in southern Finland when considering length scales of the order of 100–200 km. Owing to the location even farther from the auroral region, a similar result is evident for southern Sweden. A practical consequence of this is that even a single magnetometer located close to Simpevarp-2 would provide good estimates of GIC there. However, the calculation results presented in this paper show that a reasonable modeling of GIC is possible even though the closest magnetometers are located in Brorfelde and Uppsala (see Figure 3). A new magnetometer is being installed in Växjö, Sweden. It is located about 120 km from Simpevarp-2 and 30 km east of station Alvesta (site 2 in Figure 3). With this magnetometer we expect to get a better accuracy of the magnetic field and electric field.

[40] In this study we use a simple two-layered Earth model. This is reasonable since GIC at a given site is not only related to the local electric field at the same site, but to the regional average. To obtain the voltages, driving GIC in the network, the electric field is integrated along the paths defined by the transmission lines. Since this is a spatially smoothing operation, small-scale Earth conductivity anomalies are not significant. Also, for GIC at any given site, it is not necessary to know the electric field in very distant regions, but the nearest part of the network is dominating [see *Pirjola*, 2005b].

[41] In the future, we plan to improve the GIC model. This includes a refinement of the conductivity model of the Earth and the incorporation of data from the new magnetometer in Växjö. So far we have basically ignored the lower voltage grids (130 and 220 kV) when considering GIC in the 400 kV network. At the next stage we plan to estimate the effects of the lower voltage systems on GIC magnitudes more precisely. A final aim is to include all relevant voltage levels accurately in the GIC computations. An extension to other parts of the Swedish high-voltage system is also straightforward. Combining the GIC calculation with solar observations and space weather forecasting will enable the development of a GIC warning service to the power industry [*Wintoft*, 2005].

[42] **Acknowledgments.** We wish to thank Sture Lindahl (Gothia Power AB, Lund, Sweden) for useful discussions and advice about power grid modeling in GIC calculations. We are grateful to ELFORSK, E.ON, and Svenska Kraftnät (SVK) for supporting our studies and for providing power grid data to us. This study is partly included in the ESA pilot project SDA, ''Real-time forecast service for geomagnetically induced currents,'' supported by ESA and ELFORSK. That study was a joint collaboration between the Swedish Institute of Space Physics (IRF) and the Finnish Meteorological Institute (FMI). We also thank all institutes providing magnetometer data to IMAGE and INTERMAGNET.

References

Amm, O. (1997), Ionospheric elementary current systems in spherical coordinates and their application, *J. Geomagn. Geoelectr.*, *49*(7), 947–955.

Bolduc, L. (2002), GIC observations and studies in the Hydro-Québec power system, *J. Atmos. Sol. Terr. Phys.*, *64*(16), 1793–1802.

Boteler, D. H., and R. Pirjola (1998), Modelling geomagnetically induced currents produced by realistic and uniform electric fields, *IEEE Trans. Power Delivery*, *13*(4), 1303–1308.

Elovaara, J., P. Lindblad, R. Pirjola, S. Larsson, and B. Kielén (1992), Geomagnetically induced currents in the Nordic power system and their effects on equipment, control, protection and operation, paper presented at CIGRE Session 1992, Int. Counc. on Large Electr. Syst., Paris.

Erinmez, I. A., J. G. Kappenman, and W. A. Radasky (2002a), Management of the geomagnetically induced current risks on the national grid company's electric power transmission system, *J. Atmos. Sol. Terr. Phys.*, *64*(5–6), 743–756.

Erinmez, I. A., S. Majithia, C. Rogers, T. Yasuhiro, S. Ogawa, H. Swahn, and J. G. Kappenman (2002b), Application of modelling techniques to assess geomagnetically induced current risks on the NGC transmission system, paper presented at CIGRE Session 2002, Int. Counc. on Large Electr. Syst., Paris.

Häkkinen, L., and R. Pirjola (1986), Calculation of electric and magnetic fields due to an electrojet current system above a layered earth, *Geophysica*, *22*(1–2), 31–44.

Kappenman, J. G. (1996), Geomagnetic storms and their impact on power systems, *IEEE Power Eng. Rev.*, *16*(5), 5–8.

Kappenman, J. G., and V. D. Albertson (1990), Bracing for the geomagnetic storms, *IEEE Spectrum*, *27*(3), 27–33.

Kappenman, J. G., V. D. Albertson, and N. Mohan (1981), Investigation of geomagnetically induced currents in the proposed Winnipeg-Duluth-Twin Cities 500-kV transmission line. Res. Proj. 1205-1, Final Rep. EL-1949, 171 pp., Electr. Power Res. Inst., Palo Alto, Cali.

Karsberg, A., G. Swedenborg, and K. Wyke (1959), The influences of earth magnetic currents on telecommunication lines (English edition), *Tele*, *1*, 1–21.

Lehtinen, M., and R. Pirjola (1985), Currents produced in earthed conductor networks by geomagnetically-induced electric fields, *Ann. Geophys.*, *3*, 479–484.

Lindahl, S. (2003), Effect of geomagnetically induced currents on protection systems, report, Elforsk, Stockholm, Sweden.

Lundstedt, H. (2006), The sun, space weather and GIC effects in Sweden, *Adv. Space Res.*, *37*(6), 1182–1191.

Molinski, T. S. (2002), Why utilities respect geomagnetically induced currents, *J. Atmos. Sol. Terr. Phys.*, *64*(16), 1765–1778.

Pirjola, R. (2000), Geomagnetically induced currents during magnetic storms, *IEEE Trans. Plasma Sci.*, *28*(6), 1867–1873.

Pirjola, R. (2002), Fundamentals about the flow of geomagnetically induced currents in a power system applicable to estimating space weather risks and designing remedies, *J. Atmos. Sol. Terr. Phys.*, *64*(18), 1967–1972.

Pirjola, R. (2005a), Averages of geomagnetically induced currents (GIC) in the Finnish 400 kV electric power transmission system and the effect of neutral point reactors on GIC, *J. Atmos. Sol. Terr. Phys.*, *67*(7), 701–708.

Pirjola, R. (2005b), Effects of space weather on high-latitude ground systems, *Adv. Space Res.*, *36*(12), 2231–2240, doi:10.1016/j.asr.2003.04.074.

Pirjola, R. (2008), Study of effects of changes of earthing resistances on geomagnetically induced currents in an electric power transmission system, *Radio Sci.*, *43*, RS1004, doi:10.1029/2007RS003704.

Pulkkinen, A., O. Amm, A. Viljanen, and BEAR Working Group (2003), Ionospheric equivalent current distributions determined with the method of spherical elementary current systems, *J. Geophys. Res.*, *108*(A2), 1053, doi:10.1029/2001JA005085.

Pulkkinen, A., S. Lindahl, A. Viljanen, and R. Pirjola (2005), Geomagnetic storm of 29–31 October 2003: Geomagnetically induced currents and their relation to problems in the Swedish high-voltage power transmission system, *Space Weather*, *3*, S08C03, doi:10.1029/2004SW000123.

Pulkkinen, A., R. Pirjola, and A. Viljanen (2007), Determination of ground conductivity and system parameters for optimal modeling of geomagnetically induced current flow in technological systems, *Earth Planets Space*, *59*(9), 999–1006.

Viljanen, A., and R. Pirjola (1994), Geomagnetically induced currents in the Finnish high-voltage power system: A geophysical review, *Surv. Geophys.*, *15*(4), 383–408.

Viljanen, A., H. Nevanlinna, K. Pajunpää, and A. Pulkkinen (2001), Time derivative of the horizontal geomagnetic field as an activity indicator, *Ann. Geophys.*, *19*, 1107–1118.

Viljanen, A., A. Pulkkinen, O. Amm, R. Pirjola, T. Korja, and BEAR Working Group (2004), Fast computation of the geoelectric field using the method of elementary current systems and planar Earth models, *Ann. Geophys.*, *22*, 101–113.

Viljanen, A., A. Pulkkinen, R. Pirjola, K. Pajunpää, P. Posio, and A. Koistinen (2006), Recordings of geomagnetically induced currents and a nowcasting service of the Finnish natural gas pipeline system, *Space Weather*, *4*, S10004, doi:10.1029/2006SW000234.

Wallerius, A. (1982), Solen gav Sverige en strömstöt (in Swedish), *Ny Tek.*, *29*, 3.

Wintoft, P. (2005), Study of the solar wind coupling to the time difference horizontal geomagnetic field, *Ann. Geophys.*, *23*, 1949–1957.

H. Lundstedt, M. Wik, and P. Wintoft, Swedish Institute of Space Physics, Scheelevägen 17, SE-22370, Lund, Sweden. (magnus@lund.irf.se)

R. Pirjola and A. Viljanen, Finnish Meteorological Institute, P. O. Box 503, FIN-00101 Helsinki, Finland.

A. Pulkkinen, NASA Goddard Space Flight Center, Greenbelt, MD 20771, USA.